Measurement of anisotropy energy for magneto-optical media

Cite as: Journal of Applied Physics **71**, 813 (1992); https://doi.org/10.1063/1.351299
Submitted: 01 July 1991 . Accepted: 10 October 1991 . Published Online: 17 August 1998

R. A. Hajjar, T. H. Wu, and M. Mansuripur

Measurement of anisotropy energy for magneto-optical media

R. A. Hajjar, T. H. Wu, and M. Mansuripur
Optical Sciences Center, University of Arizona, Tucson, Arizona 85721

(Received 1 July 1991; accepted for publication 10 October 1991)

A technique is proposed for measuring the anisotropy energy of magneto-optical media. the technique consists of rotating a sample in a fixed external magnetic field and monitoring the extraordinary Hall effect signal of the sample. From the Hall effect signal, the angle of rotation of the sample, and the saturation magnetization of the sample (which is measured separately by a vibrating sample magnetometer), we obtain the anisotropy energy as a function of the deviation of magnetization from the easy axis. The technique is applied to multilayered Co/Pd and Co/Pt films as well as to amorphous rare-earth transition metal TbFeCo alloy films. The anisotropy constants thus obtained are compared with those obtained using other techniques such as torque magnetometry and Hall effect (or Kerr effect) measurements with applied field in the plane of the sample.

I. INTRODUCTION

Understanding the behavior of perpendicular magnetic anisotropy and its origins is important for magneto-optical recording media. In a single-crystal sample, the anisotropy energy depends on the magnetization direction relative to the crystallographic axes. This energy is known as the magnetocrystalline energy and is expressed in terms of parameters known as anisotropy constants. The anisotropy constants are coefficients of a mathematical series expansion and have no direct physical meaning except that they help us deduce the shape of the anisotropy energy surface or anisotropy energy profile. For polycrystalline films such as Co/Pd and Co/Pt multilayers or amorphous films such as TbFeCo, one would expect the anisotropy profile to be more complex than in single-crystal materials due to the random dispersion of the local anisotropy axes.[1,2] Therefore, it would be more suitable to determine the magnitude of the anisotropy energy as a function of the magnetization direction, rather than to assume *a priori* an expression for the energy with fitted parameters. In this paper, we propose a technique for obtaining the anisotropy energy profile of thin-film samples. The technique consists of rotating a sample in a fixed external magnetic field and monitoring the extraordinary Hall effect voltage of the sample. The anisotropy energy profile is computed from the Hall effect signal,[3,4] the angle of rotation of the sample, and the saturation magnetization of the sample. If necessary, the anisotropy constants are obtained by fitting the anisotropy energy profile to the standard expression for uniaxial anisotropy[5] and the results are compared with those obtained from other techniques such as torque magnetometry[6–10] and Hall effect (or Kerr effect) measurements with in-plane applied fields.[11,12] The technique is applied to several samples with different magnetic and structural properties. The effect of domain formation as a function of the applied magnetic field is also discussed.

II. TECHNIQUE

Consider a thin magnetic film with uniform magnetization **M** in a uniform magnetic field **H**. The total magnetic energy of the system consists of the anisotropy energy, the demagnetizing energy, and the external field energy:

$$E_{\text{total}}=E_{\text{anis}}+E_{\text{demag}}+E_{\text{ext}}. \tag{1}$$

We assume no prior knowledge of the form of the anisotropy energy except that it is uniaxial with the easy axis along the normal to the film plane and that it is dependent on the direction of the magnetization **M** which makes an angle θ with the easy axis as shown in Fig. 1. The demagnetizing energy density for a thin film is

$$E_{\text{demag}}=-2\pi M_s^2\sin^2\theta, \tag{2}$$

where $M_s(=|\mathbf{M}|)$ is the saturation magnetization of the film. The external field energy density is the dot product of **M** and **H**. Since α is the angle that the field ($H_{\text{appl}}=|\mathbf{H}|$) makes with the normal to the film plane, we have

$$E_{\text{ext}}=-H_{\text{appl}}M_s\cos(\theta-\alpha). \tag{3}$$

The total energy is minimized with respect to θ when

$$\frac{\partial E_{\text{total}}}{\partial\theta}=\frac{\partial E_{\text{anis}}}{\partial\theta}-2\pi M_s^2\sin 2\theta+H_{\text{appl}}M_s\sin(\theta-\alpha)=0. \tag{4}$$

We define $L(\alpha)=-H_{\text{appl}}M_s\sin(\theta-\alpha)$ as the torque per unit volume exerted on the sample by the applied field and rewrite Eq. (4) as follows:

$$\frac{\partial E_{\text{anis}}}{\partial\theta}=L(\alpha)+2\pi M_s^2\sin 2\theta. \tag{5}$$

Equation (5) gives the derivation of the anisotropy energy density in terms of $L(\alpha)$ and a demagnetizing term. Although we do not measure $L(\alpha)$ directly, we present our results in terms of the torque that would be measured with a torque magnetometer so that they can be directly compared. In addition to M_s and H_{appl}, Eq. (5) requires the

 0021-8979/92/140813-08$04.00

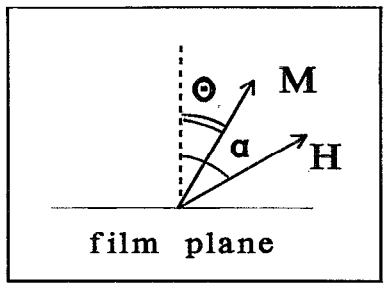

FIG. 1. M and H directions relative to the film normal.

knowledge of angles θ and α. The quantity $\cos\theta$ is obtained by measuring the Hall effect voltage as a function of α. First the sample is saturated with a perpendicular magnetic field H_{appl} (i.e., $\alpha = 0$), then it is rotated from $\alpha = 0°$ to $\alpha = 90°$ while the Hall voltage (HE_1) is being monitored. The measurement is repeated by reversing H_{appl} and measuring HE_2. The net Hall voltage (HE) is half the difference of HE_1 and HE_2 thus canceling any electronic offset. This substraction, however, does not cancel the ordinary HE which is negligible compared to the extraordinary HE.[4] An example of this measurement is displayed in Fig. 2(a) for a Co/Pt multilayered film with $H_{\text{appl}} = 20$ kOe. By normalizing the HE in Fig. 2(a) to unity at $\alpha = 0$ and taking the arc cosine {i.e., $\theta = \cos^{-1}[\text{HE}(\alpha)/\text{HE}(0)]$}, the angle θ is obtained as a function of α. $L(\alpha)$ is then computed and shown in Fig. 2(b). Figure 2(c) shows the anisotropy energy profile $E_{\text{anis}}(\theta)$ obtained by integrating Eq. (5) with respect to θ. The solid line in Fig. 2(c) represents the best match to the data with the expression $K_1 \sin^2\theta$ which is obtained when $K_1 = 3.5\times10^6$ erg/cm^3.

III. EXPERIMENTAL SETUP

We measure the Hall effect using the alternating current (ac) technique by sending a 50-Hz, 5-mA current through two point contacts located on opposite sides of a 1.5×1.5-cm^2-square sample and monitoring the Hall voltage from an orthogonal pair of point contacts using a lock-in amplifier. Since the technique requires a normalized Hall voltage as discussed above, the absolute value of the Hall resistivity is not required. The ac technique is therefore well suited for this experiment since no calibration is needed. In addition to eliminating the emf induced by the magnetic flux variations, the ac technique allows fast and reliable sampling of the Hall signal. A stepper motor (step $= 0.9°$) rotates the sample in the 5-cm air gap of an H-frame electromagnet. The maximum field capability is 20 kOe and the homogeneity of the field on the sample is $<0.25\%$ at 10 kOe. The Hall signal vs the angle of rotation of the sample is obtained for four different fields at $H = 5$, 10, 15, and 20 kOe. A personal computer controls the experiment and all the scanning and data acquisition procedures are automated.

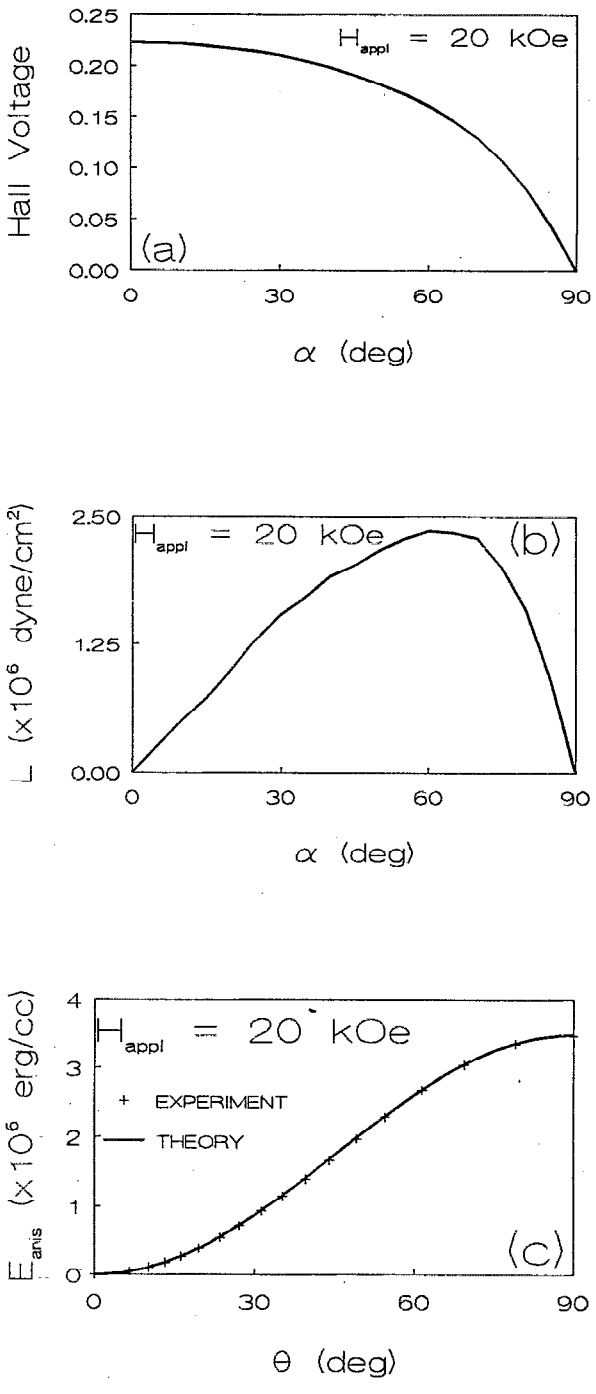

FIG. 2. Rotating sample technique performed on a Co/Pt sample with $H_{\text{appl}} = 20$ kOe. (a) Hall voltage vs angle of applied field α (deg). (b) Calculated torque $L(\alpha)$ (dyn/cm^2) vs α (deg). (c) Anisotropy energy density (erg/cm^3) vs the magnetization direction θ(deg) obtained by integrating Eq. (5) (+) and a theoretical fit of the form $K_1 \sin^2\theta$ (−) with $K_1 = 3.5\times10^6$ erg/cm^3.

IV. RESULTS

A. Co/Pt sample

The sample is a Co(0.3 nm)/Pt(1.0 nm) 30-nm-thick film evaporated on a glass substrate. The magnetic properties of the film are summarized in Table I. Figure 4(a) displays the normalized Hall effect for different values of

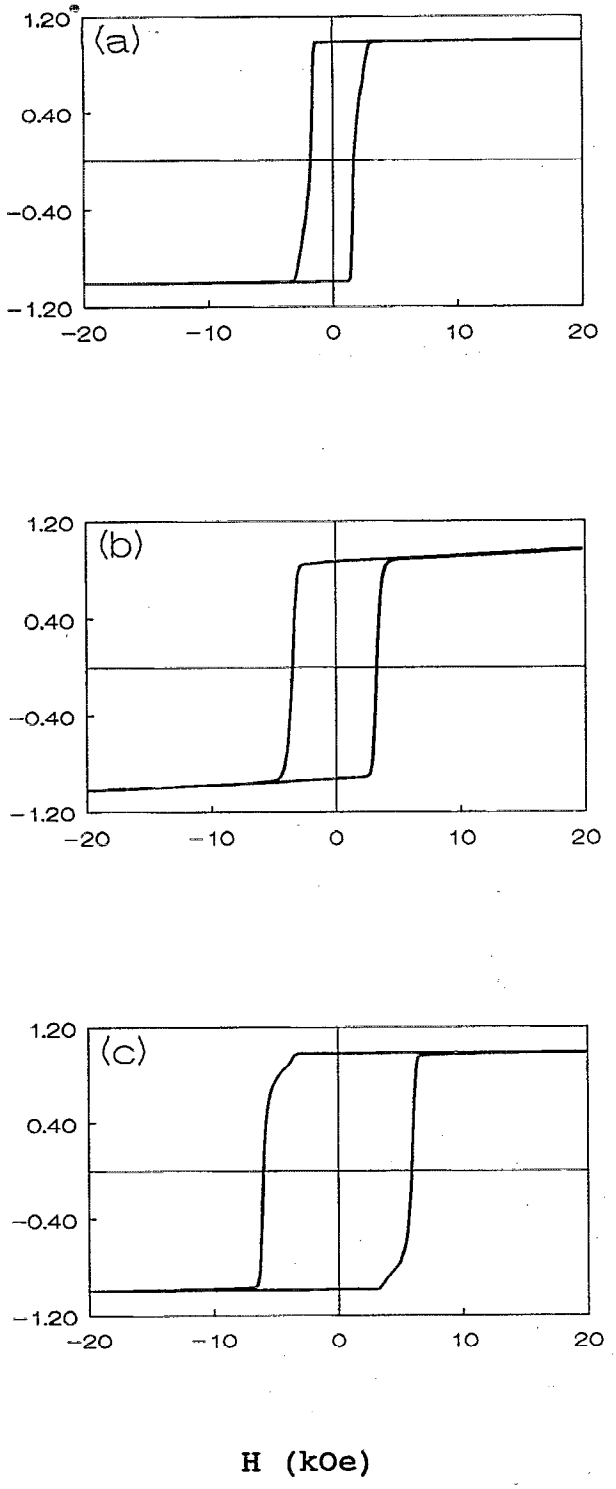

FIG. 3. Normalized Hall hysteresis loops for the three samples discussed in the paper as indicated in Table I.

the applied magnetic field. Figure 4(b) displays $E_{\text{anis}}(\theta)$ for the four measurements of Fig. 4(a). A theoretical fit (solid line) of the form $K_1 \sin^2\theta$ is superimposed on the experimental data with $K_1 = 3.5\times10^6$ erg/cm^3. When the applied magnetic field is greater than the anisotropy field $H_{\text{anis}} = 2K_1/M_s - 4\pi M_s = 11$ kOe, $E_{\text{anis}}(\theta)$ shows a perfect match to the curve of $K_1 \sin^2\theta$ and the magnetization is pulled all the way in the plane of the film [see Fig. 4(b) for $H_{\text{appl}} = 20$ and 15 kOe]. However, when H_{appl} is less than H_{anis}, for instance when H_{appl} is set to 10 or 5 kOe, the anisotropy energy profile is altered in two ways. The first effect is that the highest θ reached decreases as H_{appl} decreases. The second effect is the divergence of $E_{\text{anis}}(\theta)$ from the high field anisotropy profile beyond a certain value of θ. This divergence occurs presumably when reverse domains nucleate in the film or, irreversible changes in the state of magnetization occur. Beyond this point the expression for the demagnetizing energy [Eq. (2)] is no longer valid, but more importantly, the Hall voltage is no longer related to $\cos\theta$. Figure 4(c) is a comparison between the experimental normalized Hall voltage and the theoretical curves obtained by assuming that the sample does not demagnetize. In this simulation the value of $K_1 = 3.5\times10^6$ erg/cm^3 is used. When $H_{\text{appl}} = 20$ kOe, the magnetization follows the applied magnetic field with no signs of reverse domain formation (the same behavior is observed when $H_{\text{appl}} = 15$ kOe). When H_{appl} is equal to 10 or 5 kOe, domain formation occurs when θ is around 50° and 35°, respectively. Interestingly, domain nucleation occurs initially at a slow pace and than accelerates as the angle between **M** and **H** is increased. This might be an indication of rapid domain growth and expansion.

The same sample is measured using a torque magnetometer; the values of M_s and K_1 deduced by applying the method of Miyajima *et al.*[6] are

$$M_s = 380 \text{ emu/cm}^3,$$

$$K_1 = 3.1\times10^6 \text{ erg/cm}^3$$

with a maximum measured torque of 2.5×10^6 dyn/cm^2 when the applied field is 20 kOe. Compare this to the maximum value of 2.4×10^6 dyn/cm^2 for L found in our measurement and shown in Fig. 2(b). The measured vibrating-sample magnetometer (VSM) value of M_s is higher than that measured by the method of Miyajima *et al.* This finding is in agreement with a systematic study performed by Wielinga[7] on GdCo films where he shows a consistent reduction in the values of M_s when applying the method of Miyajima *et al.* The smaller value of M_s also affects the value found for K_1 which is strongly dependent on M_s.

The same sample is measured using an in-plane applied magnetic field ($H_{\parallel}$).[11,12] The sample is first saturated with a strong perpendicular field (at $\alpha = 0$). Then, the Hall effect and the Kerr effect signals are monitored as a function of $H_{\parallel}$ at $\alpha = 90°$. The data is normalized with respect to the height of the corresponding Hall or Kerr hysteresis loops and the direction of magnetization θ is obtained by taking the arc cosine of the normalized data. Figure 5(a) displays θ vs $H_{\parallel}$ from the Hall effect measurement which is identical to that obtained from the Kerr effect measurement. Note that up to $\theta = 20°$ the magnetization follows the field more or less coherently. This initial part of the curve is repeatable in the sense that if the field is reduced back to zero the magnetization retraces its path. Beyond $\theta = 20°$, the average magnetization direction undergoes a

TABLE I. Magnetic properties of the three samples studied. The values of M_s, H_c, and K_1 are at room temperature. The corresponding normalized Hall hysteresis loops for the three samples are displayed in Figs. 3(a), 3(b), and 3(c).

Sample	M_s (emu/cm^3) by VSM	H_c (kOe)	Normalized Hall hysteresis loop	Rotating sample technique $K_1\times10^6$ (erg/cm^3)	In-plane field technique $K_1\times10^6$ (erg/cm^3)
Co(0.3 nm)/Pt(1 nm) 30 nm	427	1.6	Fig. 3(a)	3.5	3.8
Co(0.3 nm)/Pd(0.9 nm) 12 nm	359	3.0	Fig. 3(b)	3.25	4.5
$Tb_{23}Fe_{70}Co_7$ 100 nm	95	6.2	Fig. 3(c)	4.1	4.3

rapid transition. This part of the curve is no longer repeatable indicating that domains may have formed in the sample. By further increasing $H_{\parallel}$, the magnetization everywhere (both inside and outside the domains) slowly aligns itself with the field. Given θ, the magnitude of the applied field H_{appl}, and $\alpha = 90°$, $E_{\text{anis}}(\theta)$ is obtained by integrating Eq. (5) as shown in Fig. 5(b). Since the sample demagnetizes beyond 20°, $E_{\text{anis}}(\theta)$ is only meaningful up to that point. The solid line in Fig. 5(b) is a theoretical fit to the initial part of $E_{\text{anis}}(\theta)$ with $K_1 = 3.8\times10^6$ erg/cm^3. The somewhat larger value of K_1 obtained here (compared to that obtained with the rotating sample technique) may be related to the presence of different patches with different local axes in the film. This topic will be discussed in more details in Sec. V.

B. Co/Pd sample

The sample is a Co(0.3 nm)/Pd(0.9 nm) 12-nm-thick film deposited by sputtering on a glass substrate. The magnetic properties of the sample are listed in Table I. The normalized Hall voltage curves and the corresponding anisotropy energy profiles for different values of H_{appl} are shown in Figs. 6(a) and 6(b), respectively. The solid line in Fig. 6(b) is a theoretical fit of the form $K_1 \sin^2\theta$ with $K_1 = 3.25\times10^6$ erg/cm^3. All three profiles, except for the one corresponding to $H_{\text{appl}} = 10$ kOe, are matched to the theoretical uniaxial energy expression. Following the argument presented for the Co/Pt sample, the magnetization in the sample will not reverse while rotating the sample when H_{appl} is greater than H_{anis} ($\simeq$13.5 kOe in this case). Since at $H_{\text{appl}} = 10$ kOe, the normalized Hall voltage curve shows evidence of domain formation, one might expect to see a similar behavior at $H_{\text{appl}} = 5$ kOe. However, at $H_{\text{appl}} = 5$ kOe, the sample does not reverse into domains since the normalized Hall effect curve in Fig. 6(a) shows a coherent rotation of the magnetization as a function of the applied field angle. Looking at the in-plane Hall effect measurement [Fig. 7(a)], we observe that the direction of magnetization is linear up to 7 kOe as a function of the in-plane applied field.This implies that a field of 5 kOe, applied either in the plane of the sample or rotated around the sample, will not break the sample into domains. On the other hand, for $H_{\parallel}$ greater than 7 kOe, domain nucleation and growth occurs. Therefore, this might explain why a rotating sample in a 10-kOe field breaks into domains when α approaches 90°. Finally, the integrated anisotropy energy profile for the in-plane measurement of Fig. 7(a) is shown in Fig. 7(b). The solid line in Fig. 7(b) is a theoretical match up to $\theta = 25°$ with $K_1 = 4.5\times10^6$ erg/cm^3. As in the previous example, we observe a larger anisotropy constant with the in-plane field compared to the case of a rotating sample. The reasons for this difference are discussed in Sec. V.

C. TbFeCo sample

The sample is a $Tb_{23}Fe_{70}Co_7$ 100-nm-thick film, deposited on glass by sputtering from an alloy target. The normalized Hall voltage curves and the corresponding $E_{\text{anis}}(\theta)$ for three different values of H_{appl} are displayed in Figs. 8(a) and 8(b), respectively. The solid line in Fig. 8(b) is a theoretical fit to the data with $K_1 = 4.1\times10^6$ erg/cm^3. Note that the maximum θ reached is only about 15° with $H_{\text{appl}} = 20$ kOe. Since $H_{\text{anis}} = 85$ kOe, it implies that measuring the full $E_{\text{anis}}(\theta)$ is an impossible task with the magnetic fields available to us, and that our assessment of K_1 (or higher order anisotropy constants) is limited by the extent of θ. Therefore, it would be misleading to characterize the sample with a single number such as K_1 when $E_{\text{anis}}(\theta)$ is only known up to 15°. It is more appropriate then to simply display the anisotropy energy profile in order to illustrate its shape and magnitude and the extent of θ for a given strength of the applied field. Note that for this sample the anisotropy profiles for different H_{appl} overlap with no sign of domain formation.

The anisotropy profile for this sample was also measured using an in-plane magnetic field by monitoring the Hall voltage. The magnetization direction is linearly related to $H_{\parallel}$ up to the maximum angle reached in this experiment ($\theta_{\text{max}} = 13°$) as shown in Fig. 9(a). The corresponding $E_{\text{anis}}(\theta)$ is displayed in Fig. 9(b) with a theoretical fit (solid line) corresponding to $K_1 = 4.3\times10^6$ erg/cm^3. Again this value is slightly higher than that obtained with the rotating sample technique.

V. CONCLUDING REMARKS

In this paper we studied the anisotropy energy profile of magneto-optical recording media using several tech-

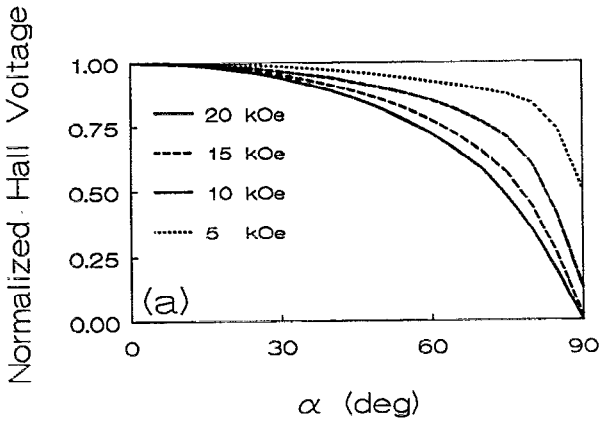

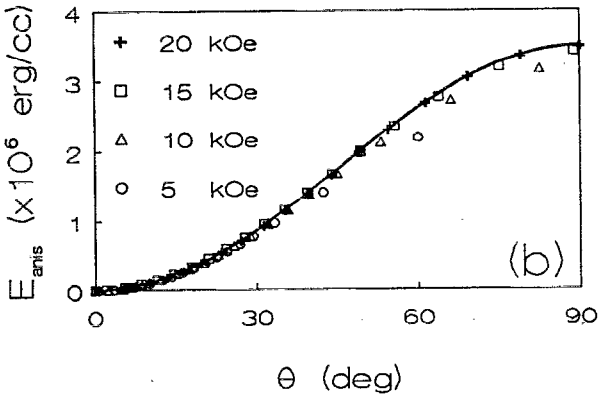

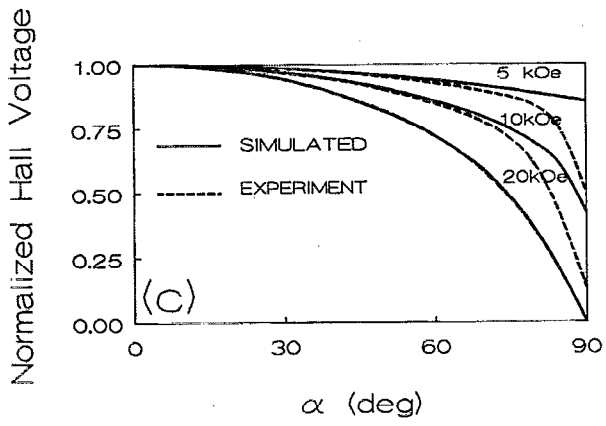

FIG. 4. Anisotropy energy measurements on a Co/Pt sample (0.3-nm-thick cobalt layers alternating with 1.0-nm-thick platinum layers, with a total thickness of 30 nm) using the rotating sample technique with different H_{appl} (kOe). (a) Normalized Hall voltage vs α (deg). (b) Anisotropy energy profiles corresponding to the data of Fig. 3(a) (+) and a theoretical fit (−) with $K_1 = 3.5\times10^6$ erg/cm^3. (c) Simulated (−) and experimental (···) normalized Hall voltage vs α (deg) for $H_{appl} = 20$, 10, and 5 kOe.

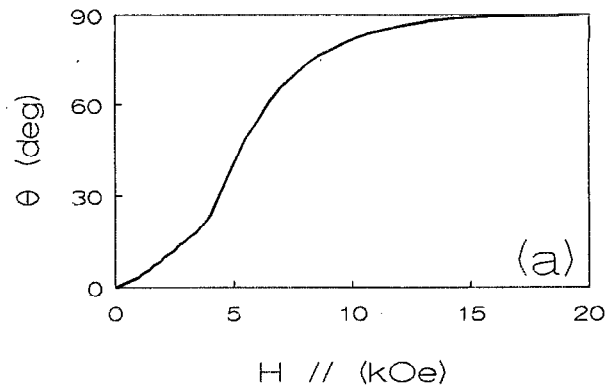

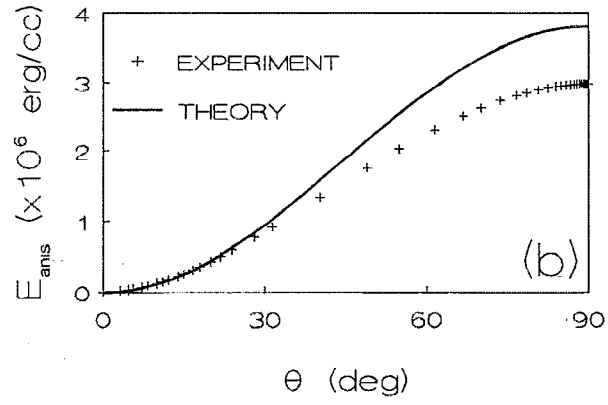

FIG. 5. Anisotropy energy measurements on a Co/Pt sample (0.3-nm-thick cobalt layers alternating with 1.0-nm-thick platinum layers, with a total thickness of 30 nm) using the in-plane field technique. (a) Magnetization direction (deg) vs in-plane applied magnetic field (kOe) obtained by taking the arc cosine of the normalized Hall voltage with respect to the height of the Hall hysteresis loop. (b) Anisotropy energy profile calculated from the measurement of Fig. 4(a) (+) and a theoretical match (−) with $K_1 = 3.8\times10^6$ erg/cm^3.

niques. The measurements are performed with different strengths of the applied magnetic field. We discuss the effect of domain formation on the anisotropy energy profile when the applied field is within a certain range. In the case of media with high anisotropy fields H_{anis}, it is important to know the upper limit of θ for which the fitted anisotropy constants are valid.

There are several differences between rotating the sample in a fixed field and applying the field either perpendicular to or in the plane of the sample. These are: (1) Larger values are deduced for the anisotropy energy with the in-plane field compared to that obtained with rotating the sample (see Table I).

(2) Films break into domains when a strong in-plane magnetic field is applied. Compare, e.g., Figs. 5(a) and 4(a) at $H_{appl} = 20$ kOe. (This behavior is typical of the multilayered Co/Pt and Co/Pd films but is also observed in some amorphous TbFeCo films.)

(3) Disagreement with the coherent rotation theory of

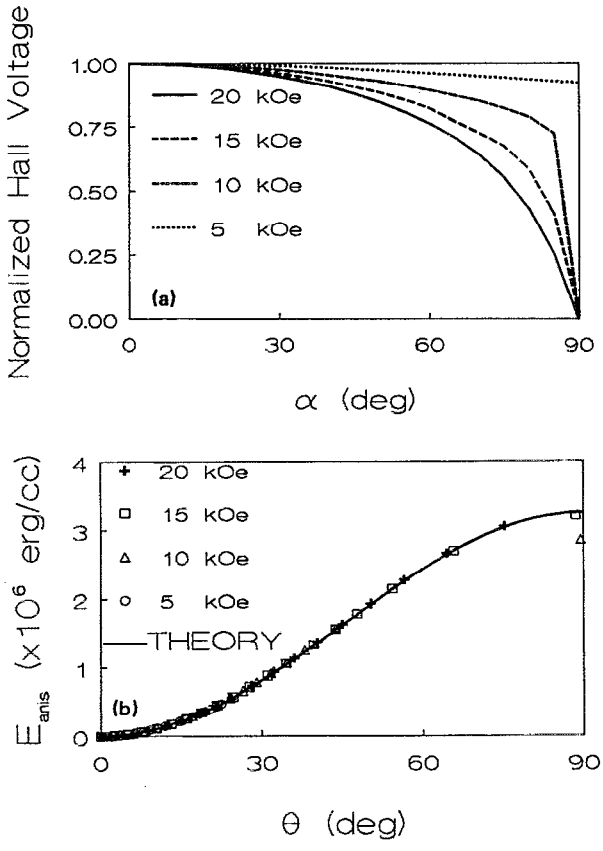

FIG. 6. Anisotropy energy measurements on a Co/Pd sample (0.3-nm-thick cobalt layers alternating with 0.9-nm-thick platinum layers, with a total thickness of 12 nm) using the rotating sample technique with different H_{appl} (kOe). (a) Normalized Hall voltage vs α (deg). (b) Anisotropy energy profiles corresponding to the data of Fig. 5(a) (+) and a theoretical fit (—) with $K_1 = 3.25 \times 10^6$ erg/cm^3.

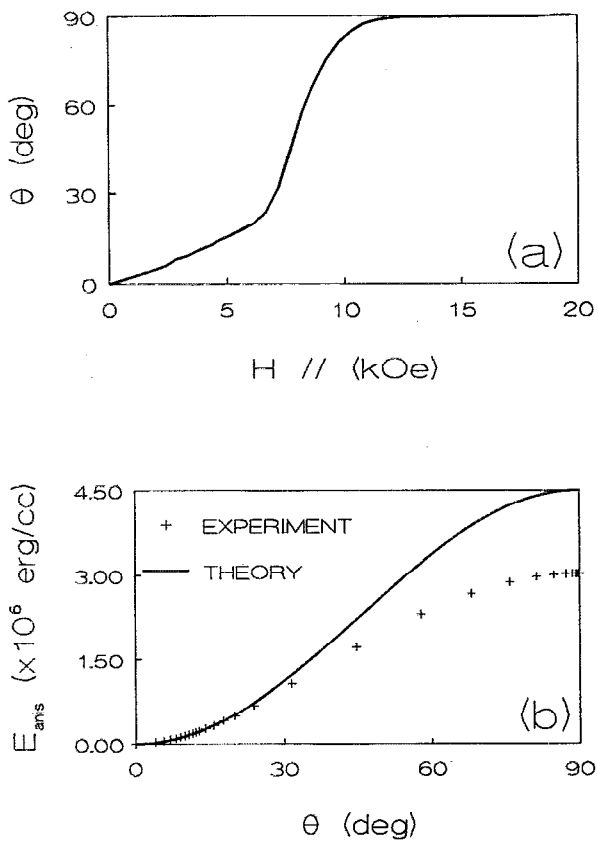

FIG. 7. Anisotropy energy measurements on a Co/Pd sample (0.3-nm-thick cobalt layers alternating with 0.9-nm-thick platinum layers, with a total thickness of 12 nm) using the in-plane field technique. (a) Magnetization direction (deg) vs in-plane applied magnetic field (kOe) obtained by taking the arc cosine of the normalized Hall voltage with respect to the height of the Hall hysteresis loop. (b) Anisotropy energy profile calculated from measurement of Fig. 6(a) (+) and a theoretical match (—) with $K_1 = 4.5 \times 10^6$ erg/cm^3.

Stoner and Wohlfarth[13] when the field is applied perpendicular to or in the plane of the sample. For instance, the loops observed experimentally deviate considerably from the calculated ones (in that case $\alpha = 0$) as shown, e.g., in Fig. 10(a) for the Co/Pt sample discussed earlier. Apart from the high squareness of the loop, the calculated coercivity is much larger than the observed one. This indicates that the easy axis magnetization reversal occurs by nucleation from defects and subsequent wall motion rather than by coherent rotation. The coercivity mechanisms have been simulated by Mansuripur and Giles[1,2] on the Connection Machine with parameters that are typical of amorphous TbFeCo films. In their simulations, they examined several hypothetical mechanisms of coercivity and found that regions of few hundred angstroms in diameter with unusually large or small magnetic parameters could act as nucleation centers and initiate the reversal process.

When the field is applied in the plane of the sample ($\alpha = 90°$) the agreement between experiment and theory is not better. Figure 10(b) shows the experimental curve of θ vs $H_{\|}$ for the Co/Pt sample and compares it with the predictions of the coherent rotation theory. In the simulations, the value of $K_1 = 3.8 \times 10^6$ erg/cm^3 is used since it matches more or less the initial part of the in-plane curve.

The fact that these films do not follow the coherent rotation theory is not surprising. These films are amorphous (in the case of TbFeCo) or polycrystalline (in the case of the Co based multilayers), and columnar grains or patches are most likely to control their magnetic properties. These patches that might be a few hundred angstroms in diameter have different magnetic parameters such as tilted axes of anisotropy and different anisotropy constants. The exchange interaction between the patches could be smaller than within the patches due to spatial gaps or segregation at the boundaries. The magnetic dipoles inside these patches interact through effective fields arising from the anisotropy field, nearest-neighbor exchange, and long-range dipole-dipole interactions. Therefore, even though the anisotropy axes are randomly tilted throughout the film, the strong exchange field gives rise to a smooth distribution of the magnetization vector across the film. This can be observed from the VSM hysteresis loop where the measured remnant magnetization is similar to the saturation magnetization. The behavior of these films can be qualitatively explained using the models that incorporate random patches.

First consider the case of a perpendicularly applied

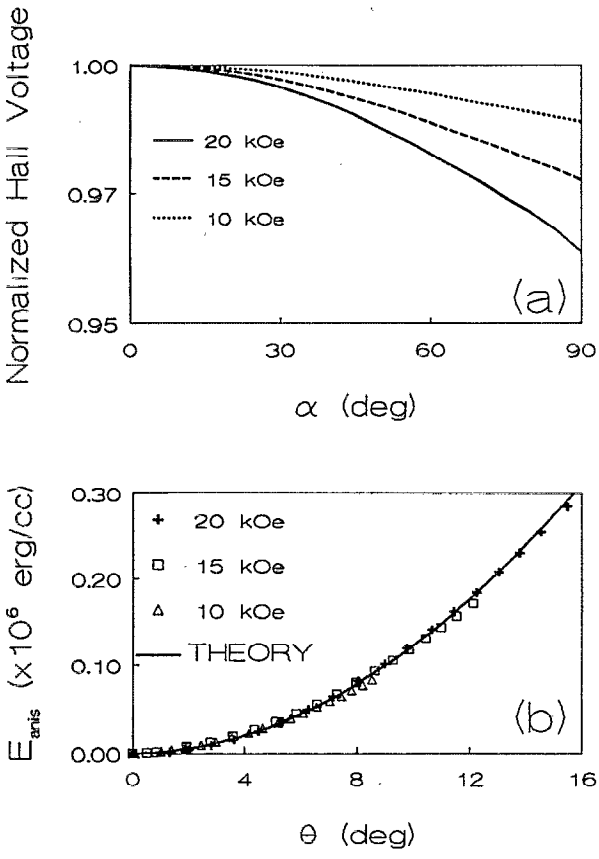

FIG. 8. Anisotropy energy measurements on a $Tb_{23}Fe_{70}Co_7$ sample 100-nm thick using the rotating sample technique with different H_{appl} (kOe). (a) Normalized Hall voltage vs α (deg). (b) Anisotropy energy profiles corresponding to the data of Fig. 7(a) (+) and a theoretical fit (−) with $K_1 = 4.1 \times 10^6$ erg/cm^3.

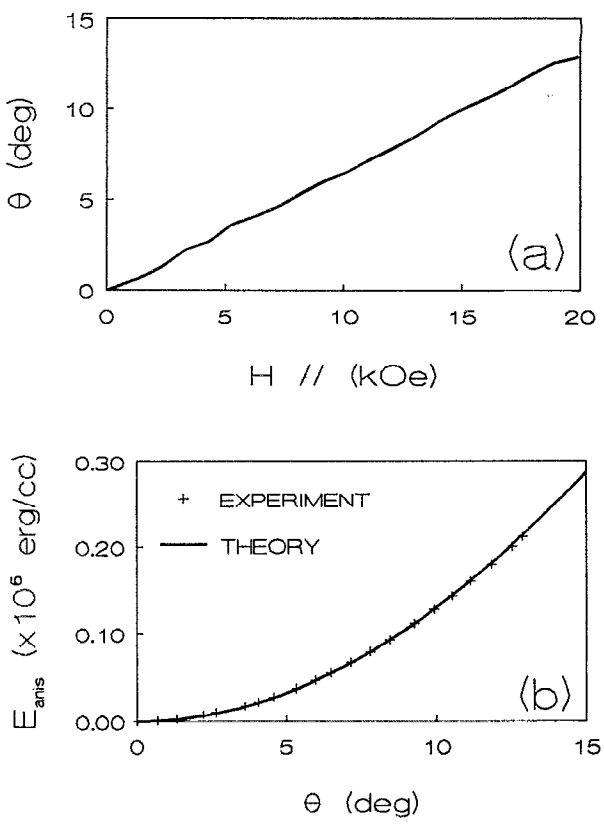

FIG. 9. Anisotropy energy measurements on a $Tb_{23}Fe_{70}Co_7$ sample 100-nm thick using the in-plane field technique. (a) Magnetization direction (deg) vs in-plane applied magnetic field (kOe) obtained by taking the arc cosine of the normalized Hall voltage with respect to the height of the Hall hysteresis loop. (b) Anisotropy energy profile calculated from the measurement of Fig. 8(a) (+) and a theoretical match (−) with $K_1 = 4.3 \times 10^6$ erg/cm^3.

magnetic field. We subject the remnant state to a reverse-magnetizing field. The dipoles corresponding to the tilted anisotropy axes with respect to the film normal or those with smaller anisotropy constants are easier to reverse than the ones corresponding to anisotropy axes normal to the film plane. These reverse-magnetized patches act as nucleation sites and grow as the field increases depending on the strength of exchange between the various patches.

Next consider rotating the sample in a strong applied field (larger than the anisotropy field). In this case the various dipoles corresponding to the tilted anisotropy axes tend to align with the applied field; the magnetization is forced to follow the applied field coherently. The measured K_1 will therefore correspond to the average bulk anisotropy of the sample. In the case of weaker applied fields the sample might undergo early reversal since the dipoles in this case are no longer aligned with the applied field. The magnetization direction corresponding to patches whose anisotropy axes are close to the film normal rather than the film plane will undergo a 180° reversal due to the demagnetizing energy; since at this point the external energy balances the anisotropy energy.

Now consider the sample in its remnant state subjected to an in-plane applied field. During the initial phase of the measurement, the dipoles corresponding to the randomly tilted anisotropy axes rotate in the direction of the applied field. Consequently, some of them are tilted closer to the film normal while others are pulled toward the plane of the film. In this part of the measurement the component of magnetization along the normal of the film is less reduced than it would be if all the axes of anisotropy were normal to the film. Therefore this behavior will yield a flatter Hall voltage as a function of the applied field and consequently a higher anisotropy energy than the one deduced from the rotating sample technique. By further increasing the applied field, the magnetization direction corresponding to patches whose anisotropy axes are inclined towards the film plane will eventually reverse. Additional increase of the field pulls the magnetization inside and outside the domains toward the in-plane direction.

We have discussed some of the possibilities that could explain the data. We showed that these magnetic systems do not obey the coherent rotation theory and that there is a lengthy list of mechanisms involved in their behavior. Our predictions await further theoretical simulations on the Connection Machine backed by experimental progress in nanomagnetics.

ACKNOWLEDGMENTS

We wish to thank Dr. T. Suzuki of IBM Almaden Research Center for interesting discussions on this subject

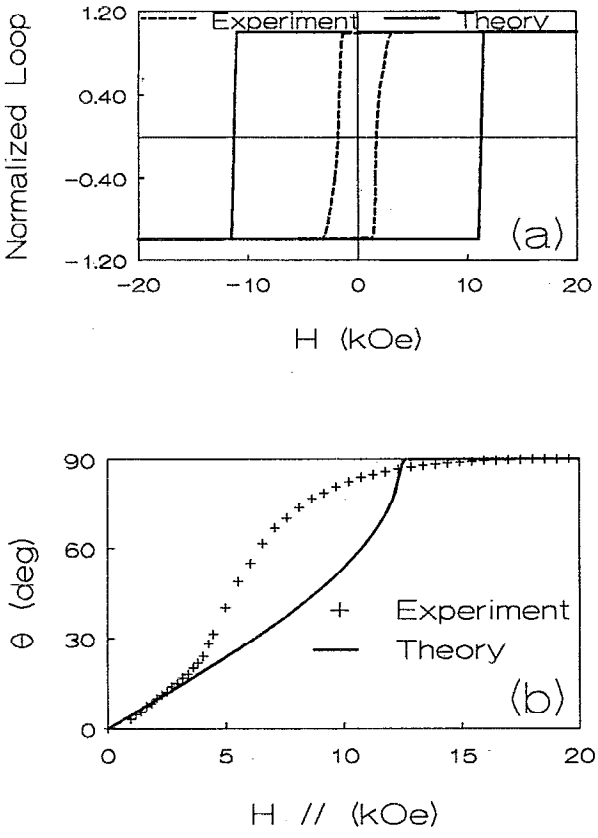

FIG. 10. (a) Simulated (−) and experimental (+) hysteresis loop. (b) Simulated (−) and experimental (+) in-plane field measurement.

and for providing us with the torque measurement data. We are also grateful to Dr. C.-J. Lin and Dr. F. Sequeda of IBM Almaden Research Center and to Dr. P. Carcia of Dupont Central Research and Development for providing the samples for this study. This work has been supported by the Optical Data Storage Center at the University of Arizona. One of us (R. A. H.) would like to acknowledge the support of an IBM fellowship.

[1] R. Giles and M. Mansuripur, Comput. Phys. March/April (1991), pp. 204–219.
[2] M. Mansuripur, R. C. Giles, and G. Patterson, J. Mag. Soc. Jpn. **15**, 17–30 (1991).
[3] T. Chen and R. Malmhall, IEEE Trans. Magn. **MAG-20**, 1025 (1984).
[4] R. Malmhall, J. Appl. Phys. **54**, 5128(1983).
[5] C. Chikazumi, *Physics of Magnetism*, edited by S. H. Charap (Wiley, New York, 1964).
[6] H. Miyajima, K. Sato, and T. Mizoguchi, J. Appl. Phys. **47**, 4669 (1976).
[7] T. Wielinga, J. Appl. Phys. **50**, 4888 (1979).
[8] K. Ishibashi, Y. Uchiyama, U. Hwang, and T. Suzuki, J. Appl. Phys. **63**, 2914 (1988).
[9] M. Tejedor, A. Fernandez, and B. Hernando, IEEE Trans. Magn. **MAG-24**, 1995 (1988).
[10] J. O. Artman, IEEE Trans. Magn. **MAG-21**, 1271 (1985).
[11] P. Wolianski, S. Chase, R. Rosenvold, M. Ruane, and M. Mansuripur, J. Appl. Phys. **60**, 346 (1986).
[12] R. Hajjar, F. L. Zhou, and M. Mansuripur, J. Appl. Phys. **67**, 5328 (1990).
[13] E. C. Stoner and E. P. Wholfarth, Philos. Trans. R. Soc. London Ser. A **240**, 599 (1948).